

Efficient numerical method for studying random walks on disordered structures

T. B. SCHRØDER^(a)

*DNRF centre “Glass and Time”, IMFUFA, Department of Sciences, Roskilde University
Postbox 260, DK-4000 Roskilde, Denmark and
Nordita - Blegdamsvej 17, DK-2100, Copenhagen Ø, Denmark*

received 20 June 2007; accepted in final form 24 November 2007
published online 19 December 2007

PACS 02.70.-c – Computational techniques; simulations
PACS 05.40.Fb – Random walks and Levy flights
PACS 66.30.Dn – Theory of diffusion and ionic conduction in solids

Abstract – A method for efficient numerical calculation of the frequency-dependent diffusion coefficient of random walks on disordered structures is presented. The method relies on solving the linear system of equations for probability currents in the frequency domain; consequently, the noise associated with traditional Monte Carlo simulation is avoided, and systems with extremely long relaxation times can be studied. Results are reported for two models on the square lattice: i) the random site-energy model and ii) a random walk at the percolation threshold for site percolation.

Copyright © EPLA, 2008

Introduction. – Random walks on disordered structures have been the subject of intense study (see, *e.g.*, refs. [1–3]), with applications ranging from systems where particles perform random walks in real space (*e.g.*, AC conduction in disordered non-metals [4–8]) to cases where the entire system is represented by a single point performing a random walk in configuration space (*e.g.*, protein-folding [9,10] and viscous liquids close to the glass transition [11–14]).

In the present letter we consider random walks in models with a finite number of states. Such a model can be considered as a network, with vertices representing states and links representing possible transitions between states. The dynamics is described by a so-called master equation [15]. The Green’s function $\mathbf{P}_{ij}(t)$ denotes the probability that the system is in state i at time t , given that it was in state j at time 0. The time development of $\mathbf{P}_{ij}(t)$ is given by the master equation

$$\frac{d}{dt} \mathbf{P}_{ij}(t) = \sum_k \mathbf{H}_{ik} \mathbf{P}_{kj}(t). \quad (1)$$

Here \mathbf{H}_{ik} is the rate of transitions from state k to state i ($i \neq k$). Conservation of probability is ensured by requiring: $\mathbf{H}_{ii} \equiv -\sum_{k \neq i} \mathbf{H}_{ki}$.

The transition rates are often “quenched” random variables. In some cases (*e.g.*, conduction in disordered solids) this reflects a real disorder in the system, in other cases (*e.g.*, protein dynamics or viscous liquid dynamics) the randomness represents *complexity*. The rationale for the latter procedure has been beautifully summarized by Wolynes [16]: Some phenomena occurring in a specific complex system are typical of those that occur in most systems chosen randomly out of an ensemble of possible systems. If this is so, the study of random systems tells us what to expect for particular complex systems.

Simulations of random walks are usually performed by Monte Carlo algorithms, see *e.g.* [17]. Briefly, the idea is the following. Suppose the system is in state k . From this state, jumps to any state i with $\mathbf{H}_{ik} \neq 0$ are possible. By suitable use of random numbers (hence the Monte Carlo name) it is possible to ensure that the “end”-state i is chosen with a probability proportional to \mathbf{H}_{ik} . The average “waiting time” at state k is $-1/\mathbf{H}_{kk}$. In this way, a “time-path” of states is generated from which any dynamical quantity (*e.g.*, a time auto-correlation function) is easily evaluated.

In many cases Monte Carlo dynamics work well. Of course, the dynamics are inherently noisy, but ensemble- and/or time-averaging reduces this noise. A more serious problem arises if the transition rates vary wildly, covering 10, 20 or more *decades*. In this case, the unlikely transitions

^(a)E-mail: tbs@ruc.dk

in practice never take place during a simulation. If some of these unlikely transitions are crucial for the long-time dynamics (*i.e.*, the system is characterized by extremely long relaxation times), even accelerated Monte Carlo methods [18–20] become inefficient; the system appears “glassy” because it is trapped in some particular region of configuration space on the time scale of the simulation.

The numerical master equation approach. – In the numerical master equation approach, dynamical properties are calculated by solving the master equation exactly, *i.e.*, dynamics of systems with arbitrarily long relaxation times can be studied, and the noise associated with Monte Carlo methods is avoided. The method is briefly reviewed in the following.

Let $\mathbf{P}(s)$ denote the Laplace transform of the matrix $\mathbf{P}(t)$ (with $s = i\omega$ being the Laplace frequency):

$$\mathbf{P}(s) = \int_0^\infty e^{-st} \mathbf{P}(t) dt \equiv L\{\mathbf{P}(t)\}.$$

The Laplace transform of the master equation (eq. (1)) is then given by (with \mathbf{I} being the identity matrix):

$$(s - \mathbf{H})\mathbf{P}(s) = \mathbf{P}(t=0) = \mathbf{I}. \quad (2)$$

Solving for $\mathbf{P}(s)$, we get

$$\mathbf{P}(s) = (s - \mathbf{H})^{-1}. \quad (3)$$

Now let \mathbf{e} and \mathbf{f} be column vectors containing the values of two physical properties, E and F , defined for the states of the model, *i.e.*, e_i is the value of E in state i . The equilibrium time correlation function $\phi_{EF}(t) \equiv \langle E(t)F(0) \rangle$ can then be expressed as (where \mathbf{P}_{eq} is the diagonal matrix with $(\mathbf{P}_{eq})_{jj}$ equal to the equilibrium probability of state j , and the superscript T denoting the transpose):

$$\phi_{EF}(t) = \sum_{ij} \mathbf{e}_i \mathbf{P}_{ij}(t) (\mathbf{P}_{eq})_{jj} \mathbf{f}_j = \mathbf{e}^T \mathbf{P}(t) \mathbf{P}_{eq} \mathbf{f}. \quad (4)$$

Taking the Laplace transform, it is found that the Laplace transform of the correlation function can be calculated numerically by $\phi_{EF}(s) = \mathbf{e}^T \mathbf{x}$, where \mathbf{x} is the solution to the matrix equation

$$(s - \mathbf{H})\mathbf{x} = \mathbf{P}_{eq} \mathbf{f}. \quad (5)$$

In many applications each state is only directly connected to a small number of other states (for a lattice this is simply the coordination number). Consequently, the matrix $(s - \mathbf{H})$ is sparse (few elements are non-zero) — a fact utilized when solving the equation numerically.

An example of a dynamic property that can be effectively calculated by the method described above is the frequency-dependent isochoric heat capacity, $C_v(s)$, which via the fluctuation-dissipation theorem [21,22] can be expressed in terms of the energy auto-correlation function, $\phi_{EE}(t) \equiv \langle E(t)E(0) \rangle$ [13]:

$$C_v(s) = -\frac{L\{\frac{d}{dt}\phi_{EE}(t)\}}{k_B T^2} = \frac{\langle E^2 \rangle}{k_B T^2} - \frac{s\phi_{EE}(s)}{k_B T^2}. \quad (6)$$

At zero frequency, $s = 0$, Einstein’s fluctuation formula is recovered: $C_v = (\langle E^2 \rangle - \langle E \rangle^2) / (k_B T^2)$. At higher frequencies the (real part of the) heat capacity will decrease, if there are parts of the system not able to respond on the time scale being probed.

The frequency-dependent diffusion coefficient. –

The frequency-dependent diffusion coefficient is defined [23] by (where $\langle \Delta x^2(t) \rangle$ is the mean-square displacement along a particular direction):

$$D(s) = s^2 L\{\langle \Delta x^2(t) \rangle\} / 2, \quad (7)$$

Note that if the system is diffusive, $\langle \Delta x^2(t) \rangle = 2Dt$, the frequency-dependent diffusion coefficient reduces to the normal diffusion constant: $D(s) = D$. If the system consists of non-interacting particles, the frequency-dependent conductivity, $\sigma(s)$, is related to $D(s)$ by the generalized Einstein relation [23]: $\sigma(s) = e^2 n \beta D(s)$, where e is the charge of the particles, n their density, and $\beta \equiv (k_B T)^{-1}$.

Equation (7) cannot be expressed in the form of the Laplace transform of eq. (4), which means that the method described in the previous section cannot be applied. Instead, eq. (7) could be evaluated by calculating $\mathbf{P}(s)$ from eq. (3), and summing the contributions from all pairs of states. Unfortunately, $\mathbf{P}(s)$ is a dense matrix (few elements are zero), so this method is only feasible for small systems. Furthermore, this method cannot give a diffusive regime ($D(s)$ approaching a positive constant for $s \rightarrow 0$) even with periodic boundary conditions applied: The minimum image convention would be needed¹, and thus the calculated mean-square displacement cannot be proportional to t at long times. These problems are partly circumvented in the so-called ACMA method, but at the expense of using the artificial “perfect electrode” boundary condition [24].

An alternative to eq. (7) is to calculate $D(s)$ from the velocity auto-correlation function [23]:

$$D(s) = L\{\langle v_x(t)v_x(0) \rangle\}, \quad (8)$$

where $v_x(t)$ is the velocity in the (arbitrarily chosen) x -direction. Applying the master equation approach to eq. (8) is, however, not straightforward since the velocity is not associated with the states, but rather with *links* connecting pairs of states with non-zero transition rates; $v_x(t) = \sum_\alpha \sum_i \Delta x_\alpha \delta(t - t_i^\alpha)$, where t_i^α is the time of the i -th jump over link α and Δx_α is the associated change in x . The δ -functions used to describe the velocities are symmetric around zero, and $L\{\delta(t)\} = 1/2$. In general, we define G to be a *link property*, if it takes on the value $\mathbf{g}_\alpha \delta(t - t')$ if the system at time t' makes a transition via link α .

¹When calculating the contribution from \mathbf{P}_{ij} , it must be assumed that the particle traveled the shortest distance between the two sites, since no information about the actual trajectory is present.

A new numerical method. – In the following we derive a method for calculating the Laplace transform of the equilibrium correlation function between two link properties G and H :

$$\phi_{GH}(s) \equiv L\{\phi_{GH}(t)\} = L\{G(t)H(0)\}. \quad (9)$$

The method is derived on a general network consisting of N states and M directional links, each connecting a pair of states, with no assumptions made about the structure of the network (see fig. 1 for a sample network). The links are defined to be directional; in the example in fig. 1 particles can jump from state “1” to state “2” via link “1”, but *not* in the opposite direction —for that a separate link would be needed. The derivation is given in two stages; In the first stage the existence of an equilibrium state is assumed, in the second stage detailed balance [$\mathbf{H}_{ik}(\mathbf{P}_{eq})_{kk} = \mathbf{H}_{ki}(\mathbf{P}_{eq})_{ii}$] is assumed.

The structure of the network is defined by two ($N \times M$) matrices \mathbf{B}^+ and \mathbf{B}^- (in the following, matrix elements for which no value is explicitly specified have the value zero, *i.e.*, the matrices are sparse):

- $\mathbf{B}_{j\alpha}^+ = 1$ if link α leads *away* from state j .
- $\mathbf{B}_{j\alpha}^- = 1$ if link α leads *into* state j .

$\mathbf{B} \equiv \mathbf{B}^- - \mathbf{B}^+$ is the “incidence matrix”, see *e.g.* [25]. We further define two ($M \times M$) diagonal matrices:

- $\mathbf{\Gamma}_{\alpha\alpha} =$ the transition rate of link α ,
- $(\mathbf{\Gamma}_{eq})_{\alpha\alpha} =$ the probability current over link α in equilibrium, *i.e.* $(\mathbf{\Gamma}_{eq})_{\alpha\alpha} = \mathbf{\Gamma}_{\alpha\alpha}(\mathbf{P}_{eq})_{jj}$ if $\mathbf{B}_{j\alpha}^+ = 1$.

The last statement can be expressed as

$$\mathbf{\Gamma}_{eq}\mathbf{B}^{+T} = \mathbf{\Gamma}\mathbf{B}^{+T}\mathbf{P}_{eq}. \quad (10)$$

We now define an ($M \times N$) matrix $\mathbf{J}(t)$, containing the conditional probability currents, *i.e.*, $\mathbf{J}_{\alpha j}(t)$ is the probability current over link α at time t , given that the system was in state j at time $t=0$. Clearly, $\mathbf{J}(t)$ is given by

$$\mathbf{J}(t) = \mathbf{\Gamma}\mathbf{B}^{+T}\mathbf{P}(t). \quad (11)$$

Expressing conservation of probability, we can write:

$$\frac{d}{dt}\mathbf{P}(t) = (\mathbf{B}^- - \mathbf{B}^+)\mathbf{J}(t) = \mathbf{B}\mathbf{J}(t). \quad (12)$$

Combining this with the time derivative of eq. (11), we get:

$$\frac{d}{dt}\mathbf{J}(t) = \mathbf{\Gamma}\mathbf{B}^{+T}\mathbf{B}\mathbf{J}(t).$$

Taking the Laplace transform gives us a matrix equation for $\mathbf{J}(s) \equiv L\{\mathbf{J}(t)\}$:

$$(s - \mathbf{\Gamma}\mathbf{B}^{+T}\mathbf{B})\mathbf{J}(s) = \mathbf{J}(t=0) = \mathbf{\Gamma}\mathbf{B}^{+T}. \quad (13)$$

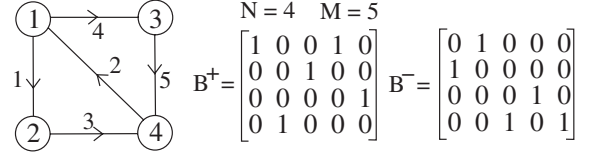


Fig. 1: Simple network with $N=4$ states, and $M=5$ directional links. The structure of the network is described by the two matrices, \mathbf{B}^+ and \mathbf{B}^- (see text).

We proceed to express the correlation function $\phi_{GH}(t)$ in terms of $\mathbf{J}(t)$. The expression for $\phi_{GH}(t)$ contains two terms: i) a term describing the contribution from two *different* transitions, one transition at time 0 and one transition at time t , and ii) a term describing the contribution to $\phi_{GH}(t=0)$ from the transition at time 0 by itself ($(\mathbf{J}(t)\mathbf{B}^-)_{\alpha\beta}$ is the rate of transitions over link α at time t , given there was a transition via link β at time zero):

$$\phi_{GH}(t) = \mathbf{g}^T\mathbf{J}(t)\mathbf{B}^-\mathbf{\Gamma}_{eq}\mathbf{h} + \delta(t)\mathbf{g}^T\mathbf{\Gamma}_{eq}\mathbf{h}.$$

Taking the Laplace transform we get

$$\phi_{GH}(s) = \mathbf{g}^T\mathbf{J}(s)\mathbf{B}^-\mathbf{\Gamma}_{eq}\mathbf{h} + \frac{1}{s}\mathbf{g}^T\mathbf{\Gamma}_{eq}\mathbf{h}. \quad (14)$$

This concludes the first stage of the derivation; combining eqs. (13) and (14) $\phi_{GH}(s)$ can be calculated.

We proceed with the second stage of the derivation where detailed balance is assumed. We consider the system as having $2M$ directional links; link $\gamma = \alpha + M$ ($1 \leq \alpha \leq M$) connects the same states as link α but in the opposite direction, *i.e.*, detailed balance can be expressed as $(\mathbf{\Gamma}_{eq})_{\gamma\gamma} = (\mathbf{\Gamma}_{eq})_{\alpha\alpha}$. The problem can now be solved by making the following substitutions expressed as block matrices:

$$\mathbf{B}^+ \rightarrow (\mathbf{B}^+ \ \mathbf{B}^-), \quad \mathbf{B}^- \rightarrow (\mathbf{B}^- \ \mathbf{B}^+), \quad (15)$$

$$\mathbf{\Gamma} \rightarrow \begin{pmatrix} \mathbf{\Gamma}^+ & \mathbf{0} \\ \mathbf{0} & \mathbf{\Gamma}^- \end{pmatrix}, \quad \mathbf{\Gamma}_{eq} \rightarrow \begin{pmatrix} \mathbf{\Gamma}_{eq} & \mathbf{0} \\ \mathbf{0} & \mathbf{\Gamma}_{eq} \end{pmatrix}, \quad (16)$$

$$\mathbf{J} \rightarrow \begin{pmatrix} \mathbf{J}^+ \\ \mathbf{J}^- \end{pmatrix}, \quad (17)$$

$$\mathbf{g} \rightarrow \begin{pmatrix} \mathbf{g} \\ -\mathbf{g} \end{pmatrix}, \quad \mathbf{h} \rightarrow \begin{pmatrix} \mathbf{h} \\ -\mathbf{h} \end{pmatrix}. \quad (18)$$

Applying these substitutions to eq. (14) we get (defining $\Delta\mathbf{J}(s) \equiv \mathbf{J}^+(s) - \mathbf{J}^-(s)$):

$$\phi_{GH}(s) = \mathbf{g}^T(\Delta\mathbf{J}(s)\mathbf{B} + \mathbf{I})\mathbf{\Gamma}_{eq}\mathbf{h}. \quad (19)$$

Applying the substitutions to eq. (13) we get two matrix equations:

$$s\mathbf{J}^+(s) - \mathbf{\Gamma}^+\mathbf{B}^{+T}\mathbf{B}\Delta\mathbf{J}(s) = \mathbf{\Gamma}^+\mathbf{B}^{+T}, \quad (20)$$

$$s\mathbf{J}^-(s) - \mathbf{\Gamma}^-\mathbf{B}^{-T}\mathbf{B}\Delta\mathbf{J}(s) = \mathbf{\Gamma}^-\mathbf{B}^{-T}. \quad (21)$$

Subtracting eq. (21) from eq. (20) we get an equation for $\Delta\mathbf{J}(s)$ (defining $\mathbf{K} \equiv \mathbf{\Gamma}^+\mathbf{B}^{+T} - \mathbf{\Gamma}^-\mathbf{B}^{-T}$):

$$(s - \mathbf{KB}) \Delta\mathbf{J}(s) = \mathbf{K}. \quad (22)$$

Solving for $\Delta\mathbf{J}(s)$ and substituting this into eq. (19), while expanding $\mathbf{I} = (s - \mathbf{KB})^{-1} (s - \mathbf{KB})$, we get

$$\phi_{GH}(s) = s\mathbf{g}^T (s\mathbf{\Gamma}_{eq}^{-1} - \mathbf{\Gamma}_{eq}^{-1}\mathbf{KB})^{-1}\mathbf{h}.$$

Applying the substitutions (eqs. (15) and (16)) to eq. (10) it is straightforward to show that $\mathbf{\Gamma}_{eq}^{-1}\mathbf{K} = -\mathbf{B}^T\mathbf{P}_{eq}^{-1}$, and thus

$$\phi_{GH}(s) = s\mathbf{g}^T \mathbf{x}, (s\mathbf{\Gamma}_{eq}^{-1} + \mathbf{B}^T\mathbf{P}_{eq}^{-1}\mathbf{B}) \mathbf{x} = \mathbf{h}. \quad (23)$$

This concludes the derivation of the method. The matrix $\mathbf{M}(s) = s\mathbf{\Gamma}_{eq}^{-1} + \mathbf{B}^T\mathbf{P}_{eq}^{-1}\mathbf{B}$ is symmetric and sparse ($\mathbf{M}_{\alpha\beta}$ is only non-zero if links α and β connects to the same state), furthermore for real $s > 0$ it is positive definite — attributes utilized when solving eq. (23) numerically.

We note that the method can be used to compute different dynamic properties at the same time. In particular, take the link property G to be the time derivative of a state-defined property, $G = \dot{E}$. It is then straightforward to show (see, *e.g.*, [26]) that

$$\phi_{GG}(t) = \phi_{\dot{E}\dot{E}}(t) = -\frac{d^2\phi_{EE}(t)}{dt^2}.$$

Taking the Laplace transform and utilizing $\langle \dot{E}E \rangle = 0$, we get

$$\phi_{GG}(s) = \phi_{\dot{E}\dot{E}}(s) = s\langle E^2 \rangle - s^2\phi_{EE}(s). \quad (24)$$

This means, *e.g.*, that if we are using the method to calculate $D(s)$ from eq. (8) by factorising the sparse matrix $\mathbf{M}(s)$, then to also calculate the frequency-dependent heat capacity using eq. (6) and eq. (24) [$C_v(s) = \phi_{\dot{E}\dot{E}}(s)/(sk_B T^2)$] simply amounts to solving for one more right-hand side, which is a negligible amount of extra work.

Applications. — We turn now to the first of two applications to illustrate the method², the random site-energy model [27,28], where independent particles undergo thermally activated hopping between nearest-neighbor lattice sites with random energies. We present results from simulations using Metropolis transition rates, on a 512×512 square lattice with periodic boundary conditions, using the box distribution for site energies, $p(E) = 1, 0 \leq E \leq 1$.

Figure 2(a) shows the real part of $D(\omega)$, calculated with the method described above³. The results are similar to

²For both models eq. (23) was solved using Matlab 6.5 on a standard PC (2.26 GHz Pentium 4).

³Using LU decomposition a frequency scan (35 frequencies) takes 216 minutes and uses 1.0 GB RAM for $L = 512$. CPU time scales as $L^{3.4}$, and memory consumption as $L^{2.0}$. At low temperatures the efficiency can be improved by removing states with so high energy that they are irrelevant for the dynamics (not done in the present work).

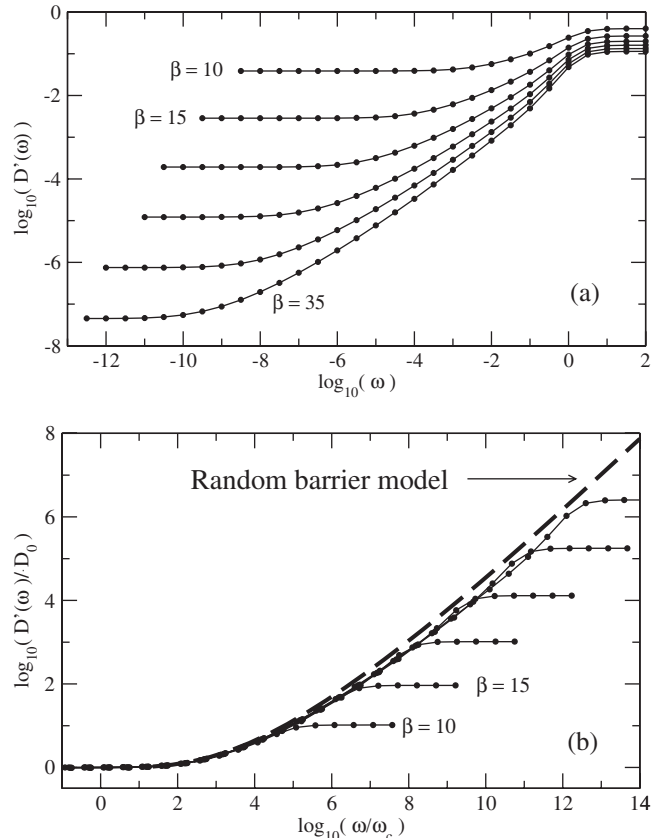


Fig. 2: (a) Real part of $D(\omega)$ for the random site-energy model on the square lattice. $\beta \equiv 1/(k_B T) = 10, 15, \dots, 35$. Data averaged over 10 independent samples. Estimated error bars are smaller than the symbols. (b) Same data scaled, with $D_0 = 1.74\beta^{0.92}\exp(-\beta E_c)$ and $\omega_c = \beta^{-2.0}\exp(-\beta E_c)$, where $E_c = p_c = 0.592746$ [7,31]. Dashed line: master curve for the random barrier model on the 2D square lattice (calculated using the method described here).

what is found for the random barrier model⁴ [7,8,29]; $D(\omega)$ is constant at high frequencies corresponding to time scales so short that only one transition can occur, and at low frequencies where the system is diffusive. Note that the dynamic range of the results is more than 14 decades — far more than what can be achieved with standard Monte Carlo methods. In fig. 2(b) the data is scaled as indicated, demonstrating collapse onto a master curve. This master curve have a slightly weaker frequency dependence than the master curve of the random barrier model. Interestingly, this is in contrast to the random site-energy model with Fermi statistics and variable range hopping, which is reported to have the *same* master curve as the random barrier model [30].

Figure 3(b) shows the imaginary part of the frequency-dependent heat capacity, $C''(\omega)$, which has a “loss peak” that moves to lower frequencies with decreasing temperature, as expected (see *e.g.*, [13]). Interestingly, while $D(\omega)$

⁴For the random barrier model, the method presented here reduces to the one described in [29].

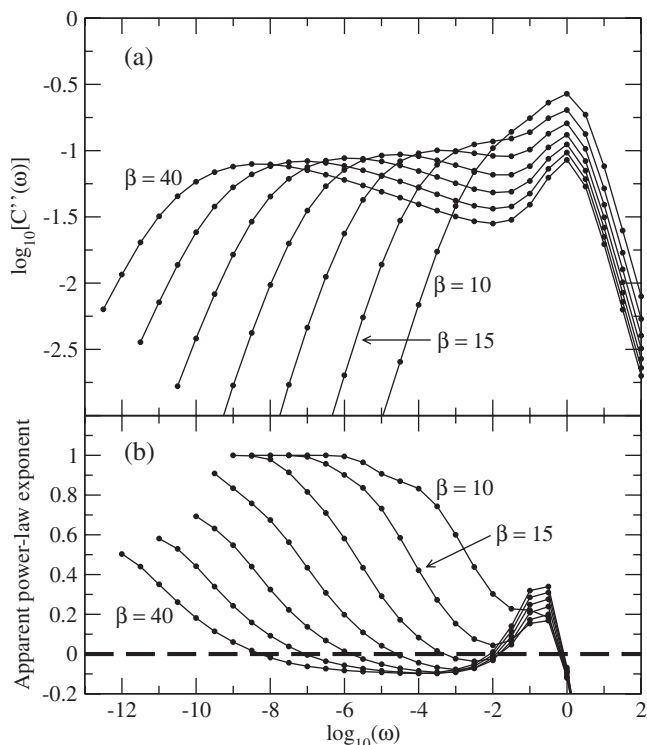


Fig. 3: (a) Imaginary part of $C(\omega)$ for the random site-energy model on the square lattice. $\beta \equiv 1/(k_B T) = 10, 15, \dots, 40$. Data averaged over 10 independent samples. Estimated error bars are smaller than the symbols. (b) Apparent power law exponent, $d \ln(C''(\omega))/d \ln(\omega)$.

can be scaled onto a master curve (fig. 2(b)), this is *not* the case for $C(\omega)$; the peaks become broader and broader as temperature is decreased. This is clearly seen in fig. 3(b) where the apparent power law exponent of $C''(\omega)$ is plotted.

Next, we consider site percolation on an $L \times L$ square lattice, at the percolation threshold, $p_c = 0.592746$ [3,31]. An ensemble of non-interacting particles performing random walks on the marked sites of the lattice (“blind ants”) will in the limit $L \rightarrow \infty$ exhibit anomalous diffusion [3,31,32]; $\langle \Delta x^2(t) \rangle \propto t^{2k}$ ($k < \frac{1}{2}$). Using eq. (7), this corresponds to $D(s) \propto s^{-\gamma}$, $\gamma = 1 - 2k$. The Alexander-Orbach (AO) conjecture predicts $k = \gamma = 1/3$, a prediction that (in contrast to other AO predictions) in the past has been found to be consistent with numerical tests (see [3] for a discussion). The latest results from Monte Carlo simulations [33] gives $k = 1/3.044 = 0.3285$, in disagreement with the AO prediction, but with no explicit error estimate given.

In fig. 4(a) we plot $D(s)$ as a function⁵ of the *real* Laplace frequency, s . The data is averaged separately over percolating and non-percolating samples, respectively (x - and y -directions are treated independently).

⁵Using Cholesky decomposition a frequency scan (35 frequencies) takes 17 minutes and uses 0.6 GB RAM for $L = 1600$. CPU time scales as $L^{2.4}$, and memory consumption as $L^{2.0}$.

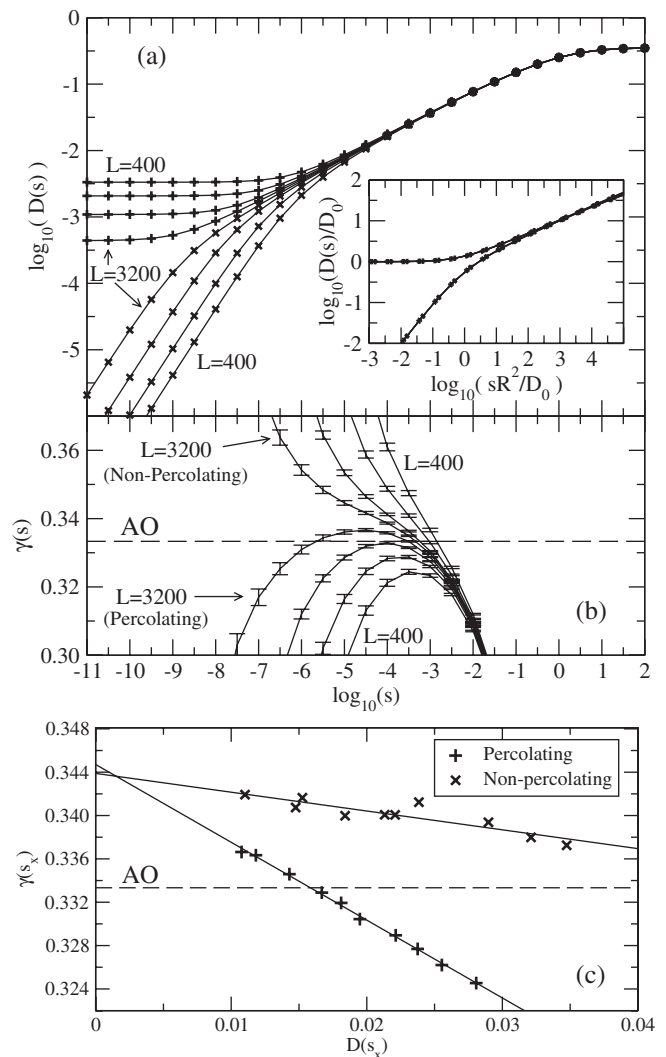


Fig. 4: (a) $D(s)$ at the percolation threshold, for system sizes $L = 400, 640, 1280$, and 3200 with periodic boundary conditions, averaged separately over percolating (+) and non-percolating samples (x). Data averaged over 1000 independent samples, except $L = 3200$ where 350 samples was used. Estimated error bars are smaller than the symbols. Inset: same data scaled as indicated. (b) Apparent power law exponent, $\gamma(s) \equiv d \ln(D(s))/d \ln(s)$. The dashed line marked “AO” indicates the Alexander-Orbach conjecture; $\gamma = 1/3$ [3]. (c) $\gamma(s_x)$ vs. $D(s_x)$, where s_x is the frequency where $\gamma(s)$ has a maximum for percolating samples, and an inflexion point for non-percolating samples.

Percolating samples have a diffusive regime, $D(s \rightarrow 0) = D_0$. The expected size dependence is $D_0 \propto L^{-t/\nu}$, with $t/\nu = 0.9825 \pm 0.0008$ [34]. In reasonable agreement with this we find $t/\nu = 0.975 \pm 0.006$. For non-percolating samples $\langle \Delta x^2(t \rightarrow \infty) \rangle$ approaches a constant, so $D(s \rightarrow 0) = sR^2$. The expected behavior is $R^2 \propto L^{\kappa/\nu}$ with $\kappa/\nu = 1.896$ [3,31], consistent with our finding $\kappa/\nu = 1.90 \pm 0.02$. The inset in fig. 4(a) shows $D(s)$ scaled onto master curves.

In fig. 4(b) we plot the apparent power law exponent, $\gamma(s) \equiv d \ln(D(s))/d \ln(s)$ (calculated *without* taking finite

differences⁶). For the percolating samples, $\gamma(s)$ passes through a maximum at $s = s_x$, while for non-percolating samples there is an inflexion point at $s = s_x$. In both cases, the increase in L causes $\gamma(s)$ to become less frequency dependent around s_x , thus indicating an approach to a true power law. $\gamma(s_x)$ is plotted as a function of $D(s_x)$ in fig. 4(c). The indicated linear extrapolations to $D(s_x) = 0$ (and thus $L = \infty$) lead to the estimate $\gamma = 0.344 \pm 0.002$ corresponding to $k = 0.328 \pm 0.001$, consistent with [33]. In particular, the finite-size scaling presented in figs. 4(b) and (c) clearly disproves the AO conjecture, $k = \gamma = 1/3$.

Conclusion. – A new numerical method for studying random walks on disordered structures has been presented. The computational cost of the method depends on the size and structure of the network representing the model. The random site-energy model is a good example of a model where the method is efficient; at low-temperatures transition rates vary over many orders of magnitude and Monte Carlo methods will be inefficient. In contrast, the percolation model has only one non-zero transition rate and the frequency dependence of $D(s)$ comes from the fractal structure of the network. In this case the advantage of the method is its ability to get the full dynamics with a single method, as well as avoiding the noise associated with Monte Carlo methods (error bars in fig. 4 indicate sample-to-sample fluctuations).

This work was supported by a grant from the Danish National Research Foundation for funding the DNRF centre for viscous liquid dynamics “Glass and Time”. The author wishes to thank J. C. DYRE, N. L. ELLEGAARD, and N. BAILEY for fruitful discussions.

REFERENCES

- [1] BOUCHAUD J.-P. and GEORGES A., *Phys. Rep.*, **195** (1990) 127.
- [2] ISICHENKO M. B., *Rev. Mod. Phys.*, **64** (1992) 961.
- [3] HUGHES B. D., *Random Walks and Random Environments* (Oxford Science Publications, Oxford) 1996.
- [4] SCHER H. and MONTROLL E. W., *Phys. Rev. B*, **12** (1975) 2455.
- [5] HAUS J. W. and KEHR K. W., *Phys. Rep.*, **150** (1987) 263.
- [6] DYRE J. C., *J. Appl. Phys.*, **64** (1988) 2456.
- [7] DYRE J. C. and SCHRØDER T. B., *Rev. Mod. Phys.*, **72** (2000) 873.
- [8] SCHRØDER T. B. and DYRE J. C., *Phys. Rev. Lett.*, **84** (2000) 310; *Phys. Chem. Chem. Phys.*, **4** (2002) 3173.
- [9] CIEPLAK M., HENKEL M., KARBOWSKI J. and BANAVAR J. R., *Phys. Rev. Lett.*, **80** (1998) 3654.
- [10] KACHALO S., LU H.-M. and LIANG J., *Phys. Rev. Lett.*, **96** (2006) 058106.
- [11] BRAWER S. A., *J. Chem. Phys.*, **81** (1984) 954.
- [12] RICHERT R. and BÄSSLER H., *J. Phys.: Condens. Matter*, **2** (1990) 2273.
- [13] NIELSEN J. K. and DYRE J. C., *Phys. Rev. B*, **54** (1996) 15754.
- [14] ANGELANI L., PARISI G., RUOCCO G. and VILIANI G., *Phys. Rev. E*, **61** (2000) 1681.
- [15] VAN KAMPEN N. G., *Stochastic Processes in Physics and Chemistry* (North-Holland, Amsterdam) 1981.
- [16] WOLYNES P. G., *Acc. Chem. Res.*, **25** (1992) 513.
- [17] BINDER K., *Rep. Prog. Phys.*, **60** (1997) 487.
- [18] BORTZ A. B., KALOS M. H. and LEBOWITZ J. L., *J. Comput. Phys.*, **17** (1975) 10.
- [19] GILLESPIE D. T., *J. Phys. Chem.*, **81** (1977) 2340.
- [20] GIBSON M. A. and BRUCK J., *J. Phys. Chem. A*, **104** (2000) 1876.
- [21] KUBO R., *J. Phys. Soc. Jpn.*, **12** (1957) 1203.
- [22] DOI M. and EDWARDS S. F., *Theory of Polymer Dynamics* (Oxford University Press, Oxford) 1986.
- [23] SCHER H. and LAX M., *Phys. Rev. B*, **7** (1973) 4491; 4502.
- [24] DYRE J. C., *Phys. Rev. B*, **49** (1994) 11709.
- [25] KORTE B. and VYGEN J., *Combinatorial Optimization: Theory and Algorithms* (Springer) 2006.
- [26] HANSEN J. P. and McDONALD I. R., *Theory of Simple Liquids*, 2nd edition (Academic Press, New York) 1986.
- [27] RINN B., BRAUNSCHWEIG U., MAASS P. and SCHIRMACHER W., *Phys. Status Solidi B*, **218** (2000) 93.
- [28] MAASS P. and RINN B., *Philos. Mag. B*, **81** (2001) 1249.
- [29] SCHRØDER T. B., *Hopping in disordered media: A model glass former and a hopping model*, PhD Thesis (Roskilde University) 1999, cond-mat/0005127.
- [30] PASVEER W. F., BOBBERT P. A. and MICHELS M. A. J., *Phys. Rev. B*, **74** (2006) 165209.
- [31] STAUFFER D. and AHARONI A., *Introduction to Percolation Theory* (Taylor and Francis, London) 1992.
- [32] METZLER R. and KLAFTER J., *Phys. Rep.*, **339** (2000) 1.
- [33] LEE S. B., *Int. J. Mod. Phys. B*, **17** (2003) 4867.
- [34] GRASSBERGER P., *Physica A*, **262** (1999) 251.

⁶From eq. (23) it can be shown that $d\phi_{GH}(s)/ds = \mathbf{g}^T \mathbf{y}$, $\mathbf{M}(s)\mathbf{y} = \mathbf{B}^T \mathbf{P}_{e_1}^{-1} \mathbf{B}\mathbf{x}$.